OPTIMUM TRAJECTORY TRACKING CONTROL OF A MULTI-ROTOR AERIAL VEHICLE

Felipe M. M. Marques

Douglas Lopes Silva

Roberto Mendes Finzi Neto

Leonardo Sanches

felipe_machini@hotmail.com

lopes.douglas@live.com

finzi@ufu.br

lsanches@ufu.br

Laboratório de Aeronaves Autônomas, Universidade Federal de Uberlândia

Av. João Naves de Ávila nº 2121 – Campus Santa Mônica, Bloco 1A, CEP 38400-902 - Minas Gerais, Brazil

Abstract. *This paper deals with the dynamical modeling of a generic multi-rotor aerial vehicle and the project of a trajectory-tracking controller using optimum modern control technique. The dynamical model is obtained from the Newton-Euler laws. The system has 6 degrees of freedom and as many inputs as the number of rotors. Further, the equations of motion are linearized around a trimmed operational condition using the small perturbation theory in order to enable the modern control techniques to be applied. The control technique concerned is the optimum LQR control approached as a servomechanism problem in order to follow a desired reference input that may be time-variant. Therefore, this technique allows the aircraft position control through velocity and attitude signals as the reference inputs. Finally, the control stability and robustness are tested via MATLAB/SIMULINK® simulations. This work was only possible thanks to FAPEMIG financial support.*

Keywords: *UAV, Multi-copter, Optimum Control, Trajectory Tracking, Dynamical Modeling*

1 INTRODUCTION

Multi-rotors are included in the category of vertical take-off and landing (VTOL) vehicles having more than two propellers. The most common configurations of these vehicles are: the tricopters (3 rotors), quadcopters (4 rotors) and hexacopters (6 rotors). As the number of rotors increases both the resulting thrust force and its corresponding payload capacity also increases, permitting a number of different maneuvers. In contrast, the aircraft construction costs and complexity also increases due to the equipment needed.

In general, the main advantages of the multi-rotors, when equipped with a fixed pitch-propeller system, are: their control simplicity, since their operational conditions (altitude, attitude and velocity) can be controlled by simply adjusting the rotational speed of each propeller independently, and their hovering ability and size, which support their miniaturization for space restricted flight missions.

As a result, the implementation of autonomous and radio controlled flights becomes favorable, including the multi-copters on the UAVs (Unmanned Aerial Vehicles) category. Nowadays, the main applications for this class of aircraft are: aerial filming/recording, surveillance, remote sensing, photogrammetry, agriculture, among others. For this reasons, it is believed that the UAVs applicability will expand even more in the next years as an indispensable device for civilian and military operations.

Also, thanks to their mechanical simplicity, simple dynamics and simple/low-cost maintenance; they are considered as being ideal robotics platform for the development and testing of control strategies (Suiçmez, 2014). Several of them were proposed and compared on multi-rotor UAVs ensuring the asymptotical stability and the ability to track pre-stablished trajectories. However, the majority uses classical control techniques (PID control) with successive loop closure which makes the design procedure increasingly difficult due to the high number of inputs and outputs of the system. Thus, for MIMO (Multiple Input Multiple Output) systems, the modern control techniques have shown to be more feasible, since the control gains can be calculated simultaneously (Stevens e Lewis, 1992).

In Bouabdallah et al. (2004), the PID and the linear quadratic regulator (LQR) guaranteed the attitude stability of a quadcopter in hovering flight. An experimental test bench with three degrees of freedom (pitch, roll and yaw angles) was built in order to validate the simulation results. Further, Raffo et al. (2008) compared the simulated and experimental results for a PID and LQR controller in UAVs used for stabilization and tracking trajectories. The two works evidence the advantages of modern over classical control techniques.

Indeed, for some applications of VTOL-UAVs it is interesting to develop a controller that is able to guide the aircraft along a pre-defined trajectory, so it can operate autonomously. In some cases, a non-linear H_∞ controller was proposed for stabilizing the rotational movements of the aircraft, while the backstepping theory minimizes the difference between the desired trajectory and the aircraft position, enabling the aircraft to track a pre-defined path (Rich, 2012).

Furthermore, concerning the trajectory tracking problem, generally, the optimum control techniques are applied considering a constant (step) input signal (Stevens e Lewis, 1992 e Suiçmez, 2014). Nevertheless, in some missions, it is desired that the aircraft is able to follow a time varying input command such that the tracking state variables have zero steady state error. In this case, the LQR controller must be treated as a servomechanism problem, where the control structure depends on the reference input signal dynamics (Lavretsky e Wise, 2013).

In this context, this present work is part of a research project from the Laboratório de Ensino em Engenharia Aeronáutica of the Universidade Federal de Uberlândia which the main goal is to develop an autonomous multi-rotor UAV civil applications. The main contribution of the paper is to use the modern control techniques to enable the aircraft to flight autonomously through a trajectory pre-defined by the user. Thus, this paper is divided according to the following sections: section 2 contains the dynamic model of the multi-copter and later the equations are linearized around the flight trimmed conditions; the LQR servomechanism problem is presented in section 3; section 4 presents the simulation results and, finally, the conclusions are outlined in section 5.

2 DYNAMICAL MODEL

The multi-copter vehicle assumes a rigid body configuration with six degrees of freedom, defining its generalized coordinate vector $\vec{q}$ as follow*:*

$$\vec{q} = \{ x \quad y \quad z \quad \theta \quad \phi \quad \psi \} \tag{1}$$

where (x, y, z) denotes the position of the center of mass of the rotorcraft with respect to the inertial frame (ICS), as shown in Fig.1, and (θ, ϕ, ψ) are the three Euler angles (roll, pitch and yaw), representing the orientation of the vehicle. Any vector, defined at the body-fixed frame (BCS), can be expressed at the ICS by using the following rotation matrix R_B^I (Valavanis, 2007),

$$\vec{r}^{\,ICS} = R_B^I \cdot \vec{r}^{\,BCS} \tag{2}$$

with, $R_B^I = R_z(\psi) R_y(\theta) R_x(\phi)$ and $R_z(\psi)$, $R_y(\theta)$ and $R_x(\phi)$ are rotations around *z*, *y* and *x* axis, respectively.

The multi-rotor equations of motion are derived using the Newton-Euler equations from the generic six degrees of freedom rigid-body system. Thus,

$$\sum F = m\vec{a} \quad \rightarrow \quad \begin{bmatrix} \sum F_x \\ \sum F_y \\ \sum F_z \end{bmatrix} = m \begin{bmatrix} \dot{u} - Rv + Qw \\ \dot{v} - Pw + Ru \\ \dot{w} - Qu + Pv \end{bmatrix} \tag{3}$$

$$\sum M = \frac{d\vec{H}}{dt} \quad \rightarrow \quad \begin{bmatrix} \sum M_x \\ \sum M_y \\ \sum M_z \end{bmatrix} = \begin{bmatrix} I_{xx}\dot{P} + QR\left(I_{zz} - I_{yy}\right) - I_{xz}(\dot{R} + PQ) \\ I_{yy}\dot{Q} + PR\left(I_{xx} - I_{zz}\right) + I_{xz}(P^2 + Q^2) \\ I_{zz}\dot{R} + PQ\left(I_{yy} - I_{xx}\right) + I_{xz}(QR + \dot{P}) \end{bmatrix} \tag{4}$$

Proceedings of the XXXVIII Iberian Latin-American Congress on Computational Methods in Engineering
P.O. Faria, R.H. Lopez, L.F.F. Miguel, W.J.S. Gomes, M. Noronha (Editores), ABMEC, Florianópolis, SC, Brazil, November 5-8, 2017.

where $F = \begin{bmatrix} F_x & F_y & F_z \end{bmatrix}$ and $M = \begin{bmatrix} M_x & M_y & M_z \end{bmatrix}$ are the external force and moment applied at the center of mass of the vehicle; both equations are written in the BCS. The (P, Q, R) are the components of the angular velocity vector defined at BCS and I_{xx}, I_{yy}, I_{zz} and I_{xz} are the components of the rotational inertia matrix of the vehicle with respect to the BCS.

Concerning the external forces, it is mainly composed of thrust, drag and gravitational components. Assuming the most commonly type of propulsion system used for UAVs (DC motors), the thrust force generated by the propeller can be considered as proportional to the propeller angular speed (Huang et al, 2009):

$$T = \left(\frac{K_\tau K_v \sqrt{2\rho\pi\beta^2}}{K_t} \Omega \right)^2 = k\Omega^2 \tag{5}$$

with K_t a proportional constant relating the torque produced by the electric motor and its electrical current, K_v relates the motor voltage and its angular velocity, K_τ is relative to the motor torque and thrust, β is the blade disc radius, ρ the density of the surrounding air and Ω the rotational velocity of the motor shaft. The thrust force T acts in the z direction of the BCS.

The drag force is due to the viscosity of the vehicle surrounding air and it can be simplified by expressing this force as being proportional to the linear velocity (Asselin, 1965) and always acting in the opposite direction of the aircraft movement. Hence, the drag force at the BCS is written as:

$$F_D^{BCS} = -k_d \vec{v}_B = \begin{bmatrix} -k_{dx} u \\ -k_{dy} v \\ -k_{dz} w \end{bmatrix} \tag{6}$$

where k_d is a friction constant which can be split in three directions of the BCS (x_B, y_B and z_B).

The gravitational force points always to the z-direction of the ICS and it is assumed as being constant since the vehicle flights at low altitude. The components of this force at the BCS is obtained from the rotation matrix, as follows:

$$F_{grav}^{BCS} = \left(R_B^I\right)^T . F_{grav}^{ICS} = \begin{bmatrix} mg\sin\theta \\ -mg\sin\phi\cos\theta \\ -mg\cos\phi\cos\theta \end{bmatrix} \tag{7}$$

Concerning the external moments acting on the vehicle, the components along yaw, pitch and roll rotations are considered. These efforts are mainly due to the propeller system actuation and on how they are distributed from the center of mass of the UAV. Figure 1 shows the arrangement of a multi-rotor propeller unit. The γ_i is the angle between the rotor's arm and the

x_B axis, l is the arm length and z_{cg} is the distance between the x_B, y_B plane and the rotor. Thus, the torque produced by the spinning propeller can be written as:

$$\tau = r \times T = r \times \sum_{i=1}^{Nm} k\Omega_i^2 \tag{8}$$

where $r = \begin{bmatrix} l\cos\gamma_i & l\sin\gamma_i & z_{cg} \end{bmatrix}$ is the vector representing the position of the rotor in the BCS.

The torques generated in the x_B, y_B and z_B directions are defined as τ_{roll}, τ_{pitch} and τ_{yaw}, respectively.

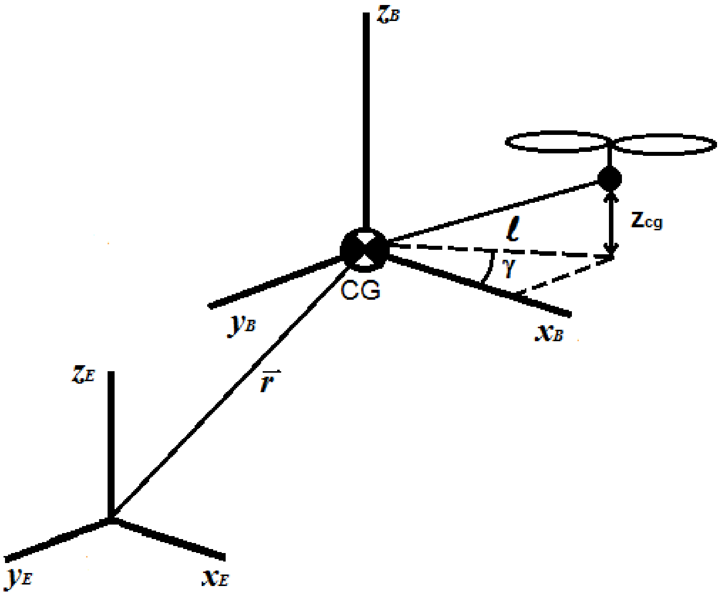

Figure 1. Multi-copter rotor position with respect to BCS and ICS.

The yaw torque τ_{yaw} is the sum of each torque generated by the spinning propellers around the z_B axis of the BCS. Mainly two components (τ_D and τ_{CD}) appear for the yaw torque. The torque τ_D is due to the air aerodynamic drag on the cross section of the blades as the vehicle rotates around its spinning axis (Asselin, 1965). The other effort, τ_{CD}, corresponds to the inertial torque produced by the angular momentum variation of the propellers (Fogelberg, 2013). Thus, the yaw torque can be written as:

$$\tau_{yaw} = \tau_D + \tau_{CD} \tag{9}$$

$$\tau_D = \frac{1}{2} R\rho C_D A v^2 \rightarrow \tau_D = \frac{1}{2} R\rho C_D A(\Omega R)^2 \rightarrow \tau_D = b\Omega^2 \tag{10}$$

Thus, the torques acting on the aircraft *CG* can be written as:

$$\begin{bmatrix} \tau_{roll} \\ \tau_{pitch} \\ \tau_{yaw} \end{bmatrix} = \begin{bmatrix} \sum_{i=1}^{Nm} kl \sin\gamma_i \Omega_i^{\,2} \\ \sum_{i=1}^{Nm} -kl\cos\gamma_i \Omega_i^{\,2} \\ \sum_{i=1}^{Nm} -b\Omega_i^{\,2} \end{bmatrix} \tag{11}$$

Afterward, since the mass of the aircraft is small, the gyroscopic effect of the blades must be accounted for in the dynamic model. This torque, calculated with respect to the CG, is generated by the change on the propellers angular momentum direction (Roskam, 2001). Assuming that the propeller blades have the same I_M and that they spin around the *z'* direction of the BCS, the gyroscopic torque produced is:

$$\tau_G = \begin{bmatrix} QI_M \sum_{i=1}^{Nm} \Omega_i \\ -PI_M \sum_{i=1}^{Nm} \Omega_i \\ 0 \end{bmatrix} \tag{12}$$

The final nonlinear equations of motion, written on the BCS, are obtained by substituting the forces and torques in the Eqs. (3) and (4):

$$m\begin{bmatrix} \dot{u} - Rv + Qw \\ \dot{v} - Pw + Ru \\ \dot{w} - Qu + Pv \end{bmatrix} = \begin{bmatrix} -k_{d\,x}u + mg\sin\theta \\ -k_{d\,y}v - mg\sin\phi\cos\theta \\ k\sum\Omega_i^2 - k_{d\,z}w - mg\cos\phi\cos\theta \end{bmatrix} \tag{13}$$

$$\begin{bmatrix} I_{xx}\dot{P} + QR\left(I_{zz} - I_{yy}\right) - I_{xz}(\dot{R} + PQ) \\ I_{yy}\dot{Q} + PR\left(I_{xx} - I_{zz}\right) + I_{xz}(P^2 + Q^2) \\ I_{zz}\dot{R} + PQ\left(I_{yy} - I_{xx}\right) + I_{xz}(QR + \dot{P}) \end{bmatrix} = \begin{bmatrix} \tau_{pitch} + QI_r\Omega_R \\ \tau_{roll} - PI_r\Omega_R \\ \tau_{yaw} \end{bmatrix} \tag{14}$$

$$\omega = \begin{bmatrix} 1 & 0 & -\sin\theta \\ 0 & \cos\phi & \cos\phi\cos\theta \\ 0 & -\sin\phi & \cos\theta\cos\phi \end{bmatrix} \dot{\Theta} \tag{15}$$

where $\Omega_R = \sum_{i=1}^{n} \Omega_i$.

The six first equations, Eqs. (13) and (14), represent the dynamic model of a hexacopter under translational and rotational movements, respectively. Equation is obtained from the kinematic relations, in which the angular velocity (Ω) on the BCS can be related to the time rate of the Euler angles $\dot{\Theta} = \begin{bmatrix} \dot{\phi} & \dot{\theta} & \dot{\psi} \end{bmatrix}^T$.

2.1 The Linearized Equations of Motion

The linearized equations of motion are necessary in order to apply modern control techniques, such as the linear quadratic regulator (LQR), to guarantee the stability and trajectory-tracking of the multi-rotor.

The procedure of linearization is based on the small perturbation theory in which the aircraft is assumed slightly perturbed from its steady operating service (trimmed condition). Since the perturbations are small, the second order terms are neglected. Thus, a general variable *g* might be expressed by:

$$f = f_0 + \tilde{f} \tag{16}$$

where f_0 is the reference trimmed value and $\tilde{f}$ is the perturbed variable. The above relation is substituted in the nonlinear equations of motions and the (~) is eliminated from the equations for the sake of simplicity. Hence, the perturbed equations of motion are:

$$\begin{aligned}
\dot{u} &= \frac{-k_{dx}}{m}u - \frac{Qw_0}{m} - \frac{Q_0 w}{m} - \frac{R_0 v}{m} + \frac{Rv_0}{m} + g\theta\cos(\theta_0) \\
\dot{v} &= \frac{-k_{dy}}{m}v + \frac{Pw_0}{m} + \frac{P_0 w}{m} - \frac{Ru_0}{m} - \frac{R_0 u}{m} - g(\phi\cos(\phi_0)\cos(\theta_0) - \theta\sin(\phi_0)\sin(\theta_0)) \\
\dot{w} &= \frac{-k_{dz}}{m}w + \frac{Qu_0}{m} + \frac{Q_0 u}{m} - \frac{Pv_0}{m} - \frac{P_0 v}{m} + \frac{2k}{m}\sum_{i=6}^{Nm}(\Omega_0\Omega_i) - g(\phi\sin(\phi_0)\cos(\theta_0) - \theta\sin(\theta_0)\cos(\phi_0))
\end{aligned} \tag{17}$$

$$\begin{aligned}
\dot{P} &= -\frac{(Q_0 R + Q R_0)(I_{zz} - I_{yy})}{I_{xx}} + \frac{Q I_M \Omega_{r_0}}{I_{xx}} + \frac{Q_0 I_M \Omega_r}{I_{xx}} + 2\sum_{i=1}^{Nm} kl \sin(\gamma_i)\Omega_{0i}\Omega_i \\
\dot{Q} &= -\frac{(P_0 R + P R_0)(I_{xx} - I_{zz})}{I_{yy}} - \frac{Q I_r \Omega_{r_0}}{I_{xx}} - \frac{Q_0 I_r \Omega_r}{I_{xx}} - 2\sum_{i=1}^{Nm} kl \cos(\gamma_i)\Omega_{0i}\Omega_i \\
\dot{R} &= -\frac{(P_0 Q + P Q_0)(I_{yy} - I_{zz})}{I_{zz}} - 2\sum_{i=1}^{Nm} b\Omega_{0i}\Omega_i
\end{aligned} \tag{18}$$

$$\begin{aligned}
\dot{\phi} &= P_0 + Q_0 \tan(\theta_0)\sin(\phi_0) + R_0 \cos(\phi_0)\tan(\theta_0) \\
\dot{\theta} &= Q_0 \cos(\phi_0) - R_0 \sin(\phi_0) \\
\dot{\psi} &= Q_0 \sin(\phi_0)\sec(\theta_0) + R_0 \sec(\theta_0)\cos(\phi_0)
\end{aligned} \tag{19}$$

In most of the applications concerning trajectory-tracking problems (Valavanis, 2007), the position of the aircraft with respect to the ICS is needed. In order to include the vehicle position as a generalized coordinate of the dynamical problem, three new relations are added to the equations of motion. They concern the linear velocities (u,v,w) that are written as a function of the temporal derivatives of (x,y,z) (Etkin, 1995) .

The set of equations, Eqs. (16-19), are given in the matrix space state form as:

$$\begin{aligned}
\dot{\vec{x}} &= A\vec{x} + B\vec{u} \\
\vec{y} &= C\vec{x} + D\vec{u}
\end{aligned} \tag{20}$$

with $\vec{y}$ being the measured signals of the dynamic system, derived from the state and input vectors. Since the measured signals are exactly the state vector, then C is an identity matrix and D is a zero matrix.

Now, the state vector $\vec{x}$ contains all the 12 generalized coordinates of the vehicle (3 spatial positions of the aircraft, 3 translational velocities in BCS, 3 angular velocities in BCS and the Euler angles) while the input vector $\vec{u}$ is composed by the angular speed of each motor of the aircraft.

The trimmed conditions of the aircraft are estimated from Eqs. (17) and (18) considering the steady operating condition, i.e., the temporal derivative terms are zero.

3 MODERN CONTROL

The modern control theory has shown to be a valuable tool in the development of autonomous systems (Suiçmez, 2014 and Hen et al., 2015). A large number of control states and inputs in the multi-copter dynamic model make difficult the application of classic control techniques such as PD and PID controllers, since the controller is based on successively closed loops. Thus, for multi-variable problems or *MIMO* (Multiple Input Multiple Output), the modern control techniques have shown to be more efficient (Kalman, 1961).

In the present paper, the linear quadratic regulator (LQR) state feedback is applied to guarantee both the stability and the trajectory-tracking capacity of the UAV. Mainly concerned with the trajectory-tracking characteristic, one defines the track error $\vec{e}(t)$ as being,

$$\vec{e}(t) = \vec{r}(\mathrm{t}) - \vec{\mathrm{x}}(\mathrm{t}) \tag{21}$$

with $\vec{r}(\mathrm{t})$ the tracking command vector containing the reference values for the states desired to be tracked.

Before designing the controller, the conditions of controllability and observability of the system have to be satisfied, according to Kalman (1961). Once these conditions are verified, the modern control technique can be applied.

The LQT (*Linear Quadratic Tracking*) controller is an extension of the LQR problem, which represents a zero order system that forces all states to the equilibrium position. Furthermore, the strategy is to increase the systems order following the internal model principle, where the error (Eq. (21)) is driven to zero. The reference input signal can be represented as a p order differential equation:

$$\overset{(p)}{r} = \sum_{i=1}^{p} a_i \overset{p-i}{r} \tag{22}$$

Now, the problem can be treated as a servomechanism design which contains the error dynamics (Eq. (22)) (Lavretsky and Wise, 2013) written as

$$\dot{z} = \tilde{A}z + \tilde{B}\mu \tag{23}$$

where the vector μ represents the plant input vector and z is the expanded state vector containing the plant and p error derivatives:

$$\dot{z} = \begin{bmatrix} e & \dot{e} & \cdots & \overset{(p-1)}{e} & x \end{bmatrix}^T \tag{24}$$

Assuming that the control law is represented by:

$$u(t) = -K_c z \tag{25}$$

Such that the feedback gain $K_c = \begin{bmatrix} K_p & K_{p-1} & \cdots & K_1 & K_x \end{bmatrix}$ is calculated in a manner that the closed loop matrix system ($\tilde{A} - \tilde{B}K_c$) is stable. The K_c matrix is obtained solving a cost-function minimization problem given by (Burns, 2001):

$$J = \int_0^{\infty} \left((z)^T Q_k (z) + \mu^T R_k \mu \right) dt \tag{26}$$

where $Q_k = Q_k^T \geq 0$, $R_k = R_k^T \geq 0$ and $\left(\tilde{A}, Q_k^{1/2}\right)$ are detectable.

Proceedings of the XXXVIII Iberian Latin-American Congress on Computational Methods in Engineering
P.O. Faria, R.H. Lopez, L.F.F. Miguel, W.J.S. Gomes, M. Noronha (Editores), ABMEC, Florianópolis, SC, Brazil, November 5-8, 2017.

Therefore, for a given space state LTI system, the LQR controller finds a gain matrix K which can minimize the cost function and bring all the states to zero simultaneously. The optimum gain matrix K is calculated using the Riccati equations (Burns, 2001) as:

$$\tilde{P}A + A^T\tilde{P} + Q_k - \tilde{P}B\tilde{R}^{-1}B^T\tilde{P} = 0 \tag{27}$$

$$K_c = -\tilde{R}_k^{-1}B^T\tilde{P} \tag{28}$$

Figure 2 illustrates the block diagram of the servomechanism system for p integrators. The control loop inside the red square represents the regulator which guarantees the states stability. On the other hand, the control loop inside the blue square contains the error integral control and that forces the position states to follow the reference input signal.

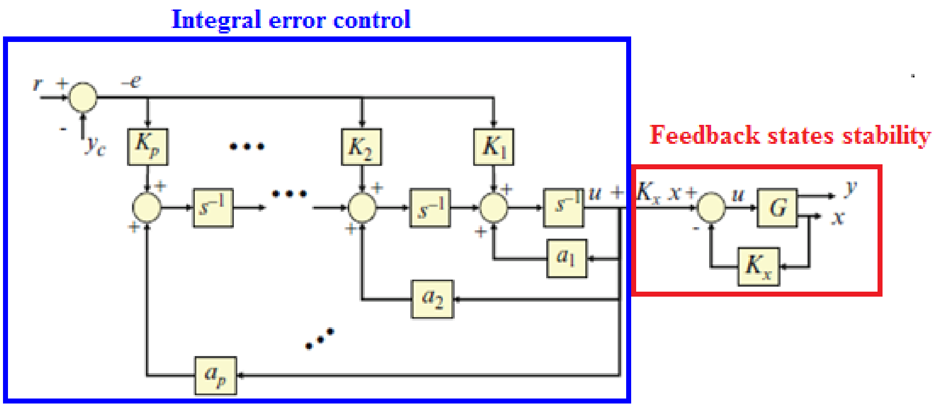

Figure 2. Servomechanism system block diagram (adapted from: Lavretsky and Wise, 2013).

4 SIMULATION AND RESULTS

In this section is discussed the main results obtained from the Matlab/Simulink® implementation of the dynamic equations. With the purpose of exemplification, a multi-rotor with six rotors (hexacopter) is assumed in the simulations. The physical parameters of the hexacopter are based on the experimental data presented in Tab. 1 (Magnusson, 2014 and Sanca et al., 2010). The dynamic simulations are performed in Matlab/Simulink®.

The k and b constants are calculated from:

$$k = \left(\frac{K_\tau K_v \sqrt{2\rho\pi\beta^2}}{K_t} \right)^2 \rightarrow k = 1.495 \cdot 10^{-05} \tag{29}$$

$$b = \frac{1}{2}\rho C_D A\beta^3 \rightarrow b = 9.46 \cdot 10^{-7} \left[kg.m^2 \right] \tag{30}$$

It is important to note that the linearized equations of motions are obtained from a hovering flight which the linear, angular velocities and Euler angles are assumed to be zero. The trimmed

Proceedings of the XXXVIII Iberian Latin-American Congress on Computational Methods in Engineering
P.O. Faria, R.H. Lopez, L.F.F. Miguel, W.J.S. Gomes, M. Noronha (Editores), ABMEC, Florianópolis, SC, Brazil, November 5-8, 2017.

rotor rotational speeds are calculated so that the propellers thrust are in equilibrium with the aircraft weight. Even the controller is designed considering the linearized equations of motion, all simulations were performed using the non-linear dynamical model plant.

Further, the simulations were performed considering that the aircraft position w.r.t the inertial coordinate frame (x_e , y_e and z_e) are the states desired to be tracked for trajectory signal as illustrated in Figs. 3 and 5. The proposed trajectory is a combination of ramp input (x_e and z_e directions) and a step input for y_e direction. The differential equations of the ramp and step reference signals are given, respectively, by:

$$\ddot{r}=0, p=2, a_1=a_2=0 \tag{31}$$

$$\dot{r}=0, p=1, a_1=a_2=0 \tag{32}$$

Thus, the state space matrix system from Eq. (20) is:

$$\tilde{A}=\begin{bmatrix} 0 & I & 0 \\ a_1 I & a_2 I & C \\ 0 & 0 & A \end{bmatrix} \quad \text{and} \quad \tilde{B}=\begin{bmatrix} 0 \\ 0 \\ B \end{bmatrix} \tag{33}$$

Table 1. Aircraft physical properties.

Property	Description	Value
m	Mass	2.326 kg
L	Hexarotor arm length	0.32 m
k_d	Drag Coefficient	4.8 10^{-2} Ns/m
I_{xx}	Moment of inertia with respect to *x* axis	0.168 kgm^2
I_{yy}	Moment of inertia with respect to *y* axis	0.168 kgm^2
I_{zz}	Moment of inertia with respect to *z* axis	0.309 kgm^2
K_v	Electric motor voltage coefficient	4.19 10^{-3} Vs/rad
K_t	Torque/current electric motor coefficient	4.19 10^{-3} Nm/A
C_Q	Thrust electric motor coefficient	1.037 10^{-3}
C_T	Torque electric motor coefficient	0.01458
G	Gravity	9.81 m/s^2
ρ	Air density	1.225 kg/m^3
B	Propeller radius	0.14 m
C_D	Propeller rotational drag coefficient	6.4 10^{-4} Ns/m

Later, the states and inputs weighting matrices $\left[Q_k\right]_{15x15}$ and $\left[R_k\right]_{6x6}$, respectively, were defined as:

$$Q = diag\left[10 \quad 10 \quad 1000 \quad 0.001 \quad 100 \quad 100 \quad 1000 \quad 1000 \quad 1000 \quad 10 \quad 10 \quad 10 \quad 10 \quad 100 \quad 1000\right] \tag{34}$$

$$R = \rho\left[I\right] \tag{35}$$

The ρ is the weighting value for the inputs μ on the cost functional (Eq. (26)).Thus, a large ρ penalizes the input vector reducing the K_c matrix gains and, consequently, slowing the system response. On the other hand, lower values of ρ grant a faster response of the system. For this simulation, the input weighting value was set as $\rho = 0.1$. The choice of the weighing values was settled after some simulations considering the best results.

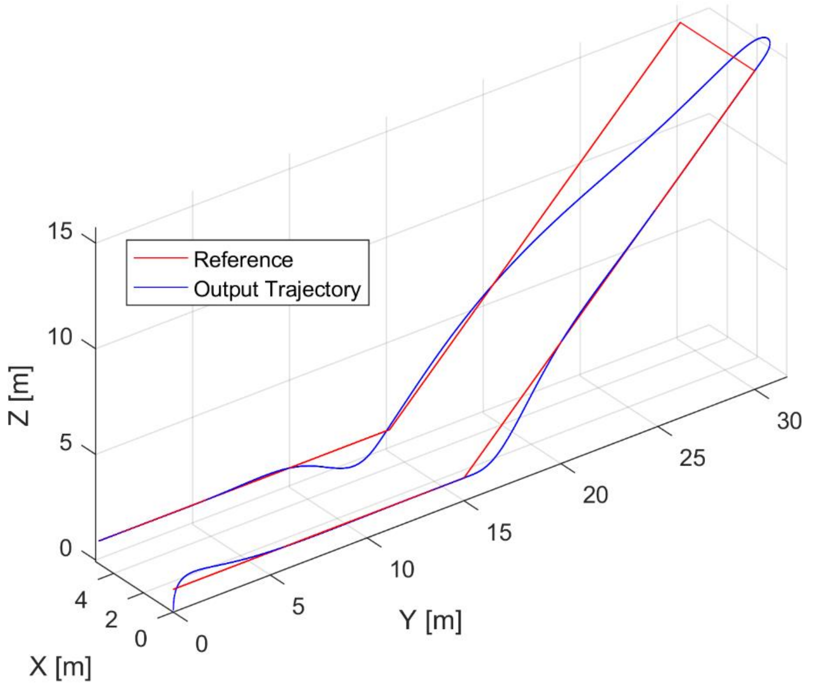

Figure 3. Simulated reference and output trajectories.

The desired reference with the simulated output trajectory is illustrated on Fig. 3 while Fig. 4 contains the aircraft path on x_e, y_e and z_e directions. From the figures, it can be inferred that the aircraft is able to complete the flight with zero final error, but the error is relatively large during the transitions as shown on Fig. 5 principally on z_e direction. Nevertheless, it can be concluded that the closed loop system is stable for this trajectory.

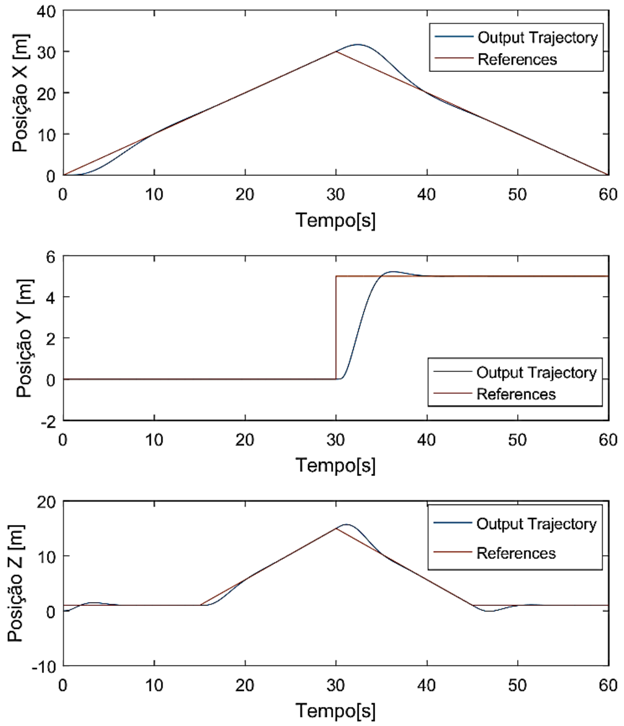

Figure 4. Hexacopter trajectories on directions x_e, y_e e z_e for $\rho = 0.1$.

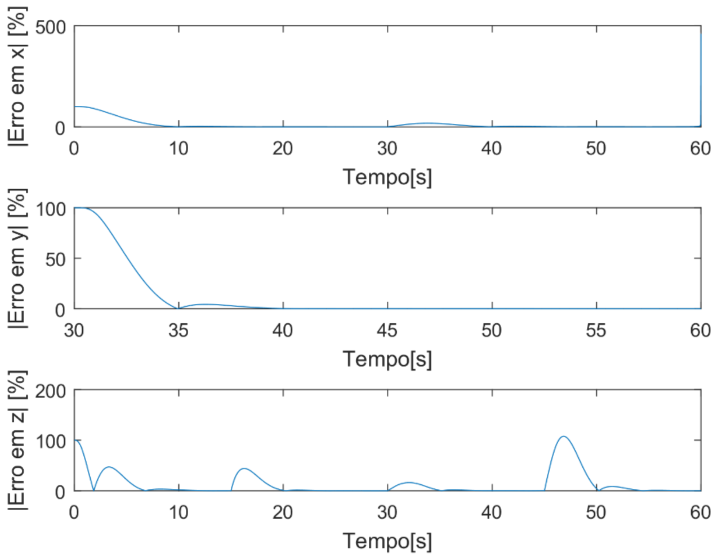

Figure 5. Position error for the simulated trajectory on x_e, y_e e z_e directions.

Finally, the control input signal variation around the trimmed condition (504.36 *rad/s*) for each of the 6 rotors can be examined on Fig. 6. It is observed that the propellers rotational speed does not exceed 545.52 *rad/s* (5209.33 *RPM*); hence, the control inputs are within the operational range for electrical DC brushless motors (7500 *RPM*) which are commonly used on UAVs.

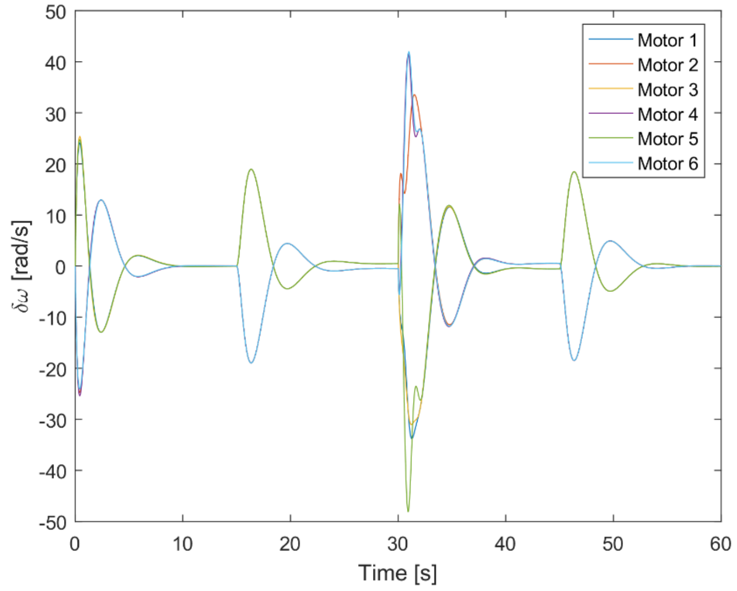

Figure 6 Input control variation for 6 rotors.

5 CONCLUSIONS

The objective of this present work was to investigate the design of a trajectory controller for a generic multi-rotor UAV aircraft via optimum control theory.

Primary, the aircraft dynamical model was obtained by the Newton-Euler equations considering the system as a rigid body with 6 degrees of freedom (3 translations and 3 rotations). The system equations of motion were validated via MATLAB/SIMULINK® simulations. Lately, the model was linearized around the hoovering condition considering the small perturbation theory, so that the modern control theories could be applied.

The LQT modern control theory was applied considering the system as a servomechanism problem. The proposed controller was structured as a regulator controller in order to keep all the states stable and an integral error controller responsible to force the error of the desired reference states to zero. In this case, the state vector was augmented in order to contain the position of the aircraft on the earth fixed inertial coordinate frame.

The feedback gain matrix is calculated using the Riccati equations that minimize a quadratic performance index function. The gain matrix and the performance index function are dependent on the weighting matrices Q_k and R_k. It was observed, during simulations, that the choice of this two matrices are crucial to the systems response, principally when the nonlinear plant model is considered.

Finally, it can be concluded that the aircraft was capable of following a desired trajectory, which was a combination of ramp, satisfactorily as show on Fig. 4 and the control effort was within the expected range. Thus, the controller is able to be applied on a real system.

For future work, the robustness of the controller can be tested for uncertain physical parameters, external perturbations and nonlinear effects in order to guarantee its performance on a real system. Also, the controller can be tested for different input signals and an optimization algorithm could be implemented in order to determine the best values for the weighting matrices for different input trajectories.

ACKNOWLEDGEMENTS

Acknowledgments

This present work was only possible thanks to FAPEMIG, CAPES and CNPQ financial support**.**

REFERENCES

Asselin, M., 1965. *An Introduction to Aircraft Performance.* Reston, Virginia: AIAA.

Bouabdallah, S., Noth, A., & Siegwart, R., 2004. PID vs LQ Control Techniques Applied to an Indoor Micro Quadrotor. *IEEE/RSJ International Conference on Intelligent Robots and Systems*, 2451-2456.

Burns, R. S., 2001. *Advanced Control Engineering.* Oxford: Plant a Tree.

Fogelberg, J., 2013. *Navigation and Autonomous Control of a Hexacopter in Indoor Environments.* Lund, Sweden: Lund University.

Huang, H., Hoffmann, G. M., Waslander, S. L. & Tomlin, C. J., 2009. *Aerodynamics and Control of Autonomous Quadrotor Helicopters in Aggressive Maneuvering*. In: *ICRA '09, International Conference on Robotics and Automation, Kobe Japan.*

Kalman, R., 1961. On the General theory of control Systems. *Proceedings of the First International Congress IFAC, Moscow 1960: Automatic and Remote Control* (pp. 481-492.. London: Butterworth & Co.

Lavretsky, E. e Wise, K. A. *Robust and Adaptive Control*. London: Springer, 2013

Magnusson, T., 2014. *Attitude Control of a Hexarotor.* Linkoping, Sweden: Linkopings Universitet.

Raffo, G. V., Ortega, M. G., & Rubio, F. R., 2008. *Backstepping/Nonlinear H Control for Path Tracking of a Quadrotor Unmanned Aerial Vehicle*. American Control Conference, 3356-3351.

Rich, M., 2012. *Model development, system identification, and control of a quadrotor helicopter.* Ames. Iowa: Iowa State University.

Roskam, J., 2001. *Airplane Flight Dynamics and Automatic Flight Controls.* Lawrence,KS: DAR Corporation.

Sanca, A. S., Laura, T. L., Cerqueira, J. J., & Alsina, P. J., 2010. Dynamic Modeling With Nonlinear Inputs and Backstepping Control for a Hexarotor Micro-Aerial vehicle. *CBA* , 1454-1461.

Stevens, B. L., & Lewis, F. L., 1992. *Aircraft Control and Simulation.* New York: Wiley-Interscience .

Suiçmez, E. C., 2014. *Trajectory Tracking of a Quadrotor Unmanned Aerial Vehicle (UAV) Via Attitude and Position Control*. Tubitak: Middle East Technical University.

Valavanis, K. P., 2007. *Advances in Unmanned Aerial Vehicles.* Dordrecht, Netherlands: Springer.